engineering proceedings

MDPI

Proceeding Paper

Investigation of the Kinetics of the Adsorption of Methylene Blue on Activated Carbon †

Nebojša Vasiljević [1,2,*], Sanja Panić [2], Goran Tadić [1], Jelena Vuković [1], Nataša Novaković [1] and Vladan Mićić [1]

[1] Faculty of Technology Zvornik, University of East Sarajevo, Karakaj 34a Zvornik, 75400 Zvornik, Bosnia and Herzegovina; goran.tadic@tfzv.ues.rs.ba (G.T.); jelena.vukovic@tfzv.ues.rs.ba (J.V.); natasaa096@gmail.com (N.N.); vladan.micic@tfzv.ues.rs.ba (V.M.)

[2] Faculty of Technology Novi Sad, University of Novi Sad, Cara Lazara 1, 21000 Novi Sad, Serbia; sanja.panic@uns.ac.rs

* Correspondence: nebojsa.vasiljevic@tfzv.ues.rs.ba

† Presented at the IX International Congress "Engineering, Environment and Materials in Process Industry"—EEM2025, Bijeljina, Bosnia and Herzegovina, 2–4 April 2025.

Abstract: This paper investigated the kinetics involved in the adsorption of methylene blue (MB) on activated carbon. Tests of the adsorbent (granulometric composition and FT-IR analyses) showed that it contains a wide range of particle sizes (5–250 μm) and that the most frequent vibrations are caused by N=C=N stretching, C=C=C stretching, metal–oxygen vibrations (e.g., Fe-O), and heteroatomic vibrations (C-Cl or C-Br). Increasing the dose of adsorbent and decreasing the initial concentration of methylene blue increases the efficiency of adsorption, while the most intensive adsorption takes up to 10 min. The adsorption process follows pseudo-second-order kinetics, which indicates that adsorption occurs due to chemical interactions between the adsorbate and adsorbent. The results indicate that the use of activated carbon achieves a high level of MB removal, especially under optimized conditions.

Keywords: activated carbon; methylene blue; adsorption kinetics; pseudo-second order; FT-IR analysis; granulometric analysis

check for updates

Academic Editors: Dragan Vujadinović, Milorad Tomić, Vesna Gojković Cvjetković, Milan Vukić, Milenko Smiljanić, Mitar Perušić and Slavko Smiljanić

Published: 9 June 2025

Citation: Vasiljević, N.; Panić, S.; Tadić, G.; Vuković, J.; Novaković, N.; Mićić, V. Investigation of the Kinetics of the Adsorption of Methylene Blue on Activated Carbon. *Eng. Proc.* **2025**, *99*, 4. https://doi.org/10.3390/engproc2025099004

Copyright: © 2025 by the authors. Licensee MDPI, Basel, Switzerland. This article is an open access article distributed under the terms and conditions of the Creative Commons Attribution (CC BY) license (https://creativecommons.org/licenses/by/4.0/).

1. Introduction

One of the most important global challenges is reducing the large amounts of pollutants in the environment caused by industrial and agricultural activities [1]. It is estimated that about 90% of water pollution is caused by organic chemicals, of which more than 50% is attributed to dyes [2]. The industries that use dyes (e.g., textile, food, paint, printing, and tanning) have the greatest harmful impact, as they continuously discharge huge amounts of dye waste into aquatic environments [3]. It is estimated that more than one million tons of textile dye waste is generated annually, of which about 30% is directly discharged into water bodies without treatment [4]. Due to the presence of dyes, the penetration of sunlight into the water is prevented, which leads to a decrease in photosynthetic activity and the death of fish and other aquatic organisms in the worst cases [5]. Dyes can prevent light from penetrating water systems, disrupting the biological activity of aquatic organisms and leading to diseases, respiratory toxicity, DNK mutation, cancer, allergies, dermatitis, skin irritation, liver and kidney damage, disorders of the central nervous system, etc. [6].

Methylene blue (MB) is a basic dye that is used in industrial activities such as the dyeing of textiles and leather, printing calico, printing cotton, and biological staining methods [7]. It belongs to the thiazine dye group, with a molecular formula of $C_{16}H_{18}ClN_3S$

and a molecular weight of 319.85 g/mol. MB has a distinct blue color and good solubility in water. It contains a positively charged cationic group, which is why it can be easily adsorbed onto materials that have a negatively charged surface [8]. Excessive doses of methylene blue have been reported to cause diarrhea, vomiting, nausea, gastritis, abdominal and chest pain, extreme headaches, a lot of sweating, mental fatigue, and methemoglobinemia [3].

A number of techniques have been suggested to remove methylene blue from wastewater. They include (a) physical methods: membrane filtration [9], ultrafiltration [10], and hollow fiber membrane contactors [11]; (b) chemical methods: coagulation [12], flocculation [13], electrochemical degradation [14], photocatalytic degradation [15], and advanced oxidation processes (AOPs) [16]; (c) biological methods: aerobic processes [17] and anaerobic processes [18]; and (d) physicochemical methods: photodegradation [19] and adsorption [20–22]. Among these techniques, adsorption has a great decontamination potential when it comes to MB. This method is a mass transfer process, in which the surface of solid adsorbents is used to accumulate a substance that is present in liquid or gaseous media [8]. Adsorption has great decontamination potential due to its tunability, versatility, and the wide variety of sorbents available [1,23]. Some other advantages include the simple operation of these processes, their low cost, the abundance of adsorbent materials, their high performance, fast recycling, and the assurance of no secondary contaminants being produced [3,24].

Activated carbon, biochar, graphene and graphene oxide, zeolites, clays, etc., can be used as adsorbents for MB removal [25–27]. The adsorbent most widely used in this area is activated carbon [28]. Activated carbon is a common term used to describe carbon-based materials that have a large surface area, a highly developed internal pore structure (consisting of pores that have a diverse size distribution), and a wide range of oxygenated functional groups present on their surface [7,29,30]. The porosity and pore volume distribution, and therefore the activity of activated carbon, depend on the activation of the carbon. There are many different activation agents, but they can be roughly divided into those that can be used for chemical activation (sodium hydroxide, potassium hydroxide, sulfuric acid, phosphoric acid) and those that can be used for physical activation (steam, air, or CO_2) [31,32].

The aim of this scientific paper is to investigate the kinetics of methylene blue adsorption onto commercial activated carbon. First, the activated carbon will be characterized in order to examine whether its properties are favorable for adsorption. After that, the influence of time, initial MB concentration, and the dose of adsorbent on the efficiency of methyl blue adsorption will be analyzed. Finally, this study will determine the reaction order, adsorption rate constant, and the equilibrium adsorption capacity of the activated carbon.

2. Materials and Methods

To investigate the adsorption of methylene blue (MB) onto activated carbon (an adsorbent), a series of experiments was performed by varying the initial concentration of the methylene blue (MB) (Lach:ner, Neratovice, Czech Republic) solution and the amount of activated carbon. First, a stock solution of MB (100 mg/L) was made, which was then diluted to 12.5 mg/L and 25 mg/L, and these diluted solutions were used in the experiments. The characterization of the activated carbon was performed using a Cary 630 FTIR Spectrometer (Agilent Technologies, Santa Clara, CA, USA)—to identify functional groups—and a Mastersizer 3000E (Malvern Panalytical, Malvern, UK)—to determine the granulometric composition. For each experiment, 0.1 dm^3 of MB solution was transferred into 300 mL plastic tubes together with defined amounts of adsorbent: 0.05 g/L, 0.10 g/L, 0.15 g/L, 0.20 g/L, or 0.25 g/L. Adsorption was carried out in a shaker at a speed of 120 rpm over different time intervals: 10, 20, 35, 60, or 90 min. The samples were filtered

after the end of adsorption and the remaining concentration of MB in the solution was determined spectrophotometrically at a wavelength of 664 nm using a Shimadzu UV-1800 spectrophotometer (Cole Parmer, Vernon Hills, IL, USA).

The efficiency of color removal (η) was determined by Equation (1) [33]:

$$\eta = \frac{C_0 - C_t}{C_0} \cdot 100 \quad (1)$$

where C_0 [mg/L] and C_t [mg/L] are the initial and remaining concentrations of methylene blue (MB).

The amount of adsorbate adsorbed per unit mass of adsorbent in time t (q_t) was determined by Equation (2) [26]:

$$q_t = \frac{(C_0 - C_t) \cdot V}{m} 100 \quad (2)$$

where m [g] and V [dm^3] are the mass of the adsorbent and the volume of the solution.

After that, the adsorption kinetics was investigated. In accordance with the literature data, adsorption can follow the pseudo-first-order or pseudo-second-order kinetic model, so in our work we examined whether the obtained results corresponded to either of the proposed kinetic models. If the adsorption follows the pseudo-first-order model, it is determined by Equation (3) [34], and if it follows the pseudo-second-order model, it is determined by Equation (4) [35]:

$$\ln(q_e - q_t) = \ln q_e - k_1 t \quad (3)$$

$$\frac{t}{q_t} = \frac{1}{k_2 q_e^2} + \frac{t}{q_e} \quad (4)$$

where q_e [mg/g], k_1 [min^{-1}], and k_2 [g/(mg·min)] represent the equilibrium adsorption capacity, pseudo-first-order rate constant, and pseudo-second-order rate constant, respectively.

All experimental research was carried out in the laboratories of the Faculty of Technology Zvornik, University of East Sarajevo. Adsorption kinetics were investigated using MS Excel, while additional statistical analysis was performed using Minitab 21.

3. Results and Discussion

3.1. Adsorbent Characterization

In order to examine the properties of the adsorbent, FT-IR and granulometric composition analyses were performed, and the obtained results are shown in Figure 1. The FT-IR analysis determined that the activated carbon used does not have many additional functional groups. First of all, a small peak related to carbodiimides (N=C=N stretching) was observed at the wave number 2150 cm^{-1}, while a peak related to allenes (C=C=C stretching) was observed at 2000 cm^{-1}. Finally, there were peaks in the region of 550–400 cm^{-1}, which are usually associated with metal–oxygen vibrations (e.g., Fe–O) or heteroatomic bonds (C-Cl or C-Br) [36].

Carbodiimides enable electrostatic interactions and hydrogen bonds with adsorbates, while allenes contribute to π-π interactions with aromatic molecules, improving the adsorption of organic pollutants. Metal–oxygen bonds, such as Fe–O or Ti–O, enable coordinative adsorption and can influence the surface charge and, in some cases, the catalytic degradation of adsorbed pollutants [37–39].

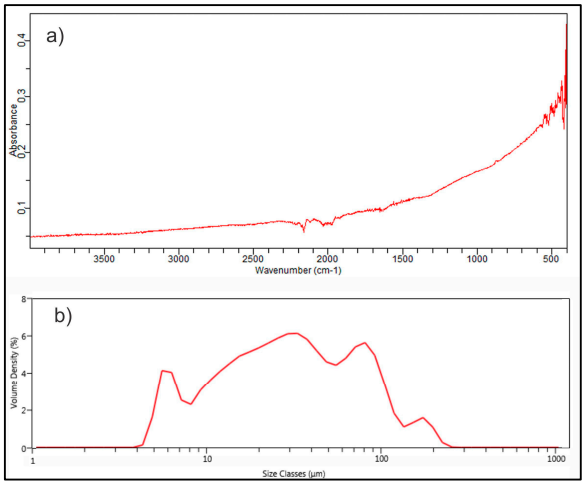


Figure 1. Characteristics of activated carbon: (**a**) FT-IR spectrum and (**b**) granulometric composition.

The laser diffraction of activated carbon determined that the total range of the particle sizes was 4–250 µm, where Dx(10) is 7.48 µm, Dx(50) = 29.4 µm, and Dx(90) = 94.3 µm. Such a wide distribution of particle sizes indicates a heterogeneous sample. The main advantages of this sample are that larger particles enable easier filtration, because the system does not clog, while smaller particles have a larger specific surface area and contribute to higher adsorption efficiency [40]. The main disadvantage of a heterogeneous system is that the smaller particles adsorb faster, and larger particles more slowly, which leads to variability in its adsorption kinetics.

3.2. Investigation of the Removal Efficiency of Methylene Blue (MB)

In order to have a clearer insight into the effectiveness of the adsorbent, a series of experiments was conducted which aimed at determining the best process conditions for the removal of MB. Figure 2 shows the efficiency of MB removal with different process parameters.

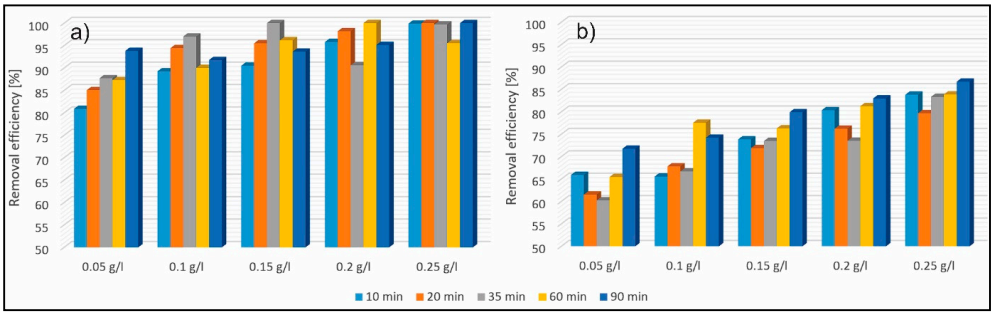


Figure 2. Removal efficiency of methylene blue (MB) via adsorption on activated carbon at two initial dye concentrations: (**a**) 12.5 mg/L and (**b**) 25 mg/L.

Depending on the initial MB concentrations, the efficiency of color removal varies. At a lower initial MB concentration (12.5 mg/L), the number of available adsorption sites on the surface of the activated carbon is greater, while at a higher initial MB concentration (25 mg/L), the available adsorption sites become saturated more quickly. Therefore, the removal efficiency is higher at a lower initial MB concentration. Normally, as the initial dye concentration increases for a fixed amount of adsorbent, the dye molecules compete for the available active sites, thereby decreasing the efficiency of their removal [8].

The concentration of the adsorbent has a greater impact on the efficiency of MB removal than the adsorption time. Looking at Figure 2a (with an initial MB concentration of 12.5 mg/L), at lower concentrations (0.05 g/L and 0.1 g/L) of the adsorbent, there was a

gradual increase in the efficiency of MB removal, while at higher doses of the adsorbent (0.15 g/L, 0.2 g/L, and 0.25 g/L), the removal efficiency was 100%. These results indicate that at lower doses of the adsorbent, there are fewer active sites available for adsorption, and therefore the adsorption process is slower [38]. The highest efficiency (100%) was achieved with 0.25 g/L of activated carbon after only 20 min and with 0.15 g/L of adsorbent after 35 min, which can be seen from Figure 2b. At a higher initial concentration of MB (25 mg/L), even the highest dose (0.25 g/L) of adsorbent did not achieve sufficient efficiency. This indicates that a larger amount of adsorbent or a longer contact time is required to achieve the same efficiency as for 12.5 mg/L of MB.

Time plays a more significant role in the adsorption process at lower adsorbent concentrations. For both concentrations, the removal efficiency increases with time, reflecting the gradual diffusion of MB molecules to the available adsorption sites. Thus, from Figure 2a it is observed that with 0.05 g/L of the adsorbent, the efficiency increased from 80.84% to 93.82% when the time was increased from 10 to 90 min. However, at 0.25 g/L (Figure 2b), almost complete removal (99.90%) was achieved after only 10 min. At higher adsorbent concentrations, equilibrium was reached after 20–35 min, after which the removal efficiency did not change significantly. Minor deviations in removal efficiency were observed, especially at intermediate times. The probable reason for this is experimental variability, i.e., errors in solution mixing or measurement errors. Despite this, the trends confirm that activated carbon is an effective adsorbent for MB.

In order to determine which of the process parameters have a greater impact on the percentage of color removed, a regression analysis was performed, and the obtained results were expressed as a Pareto chart (Figure 3).

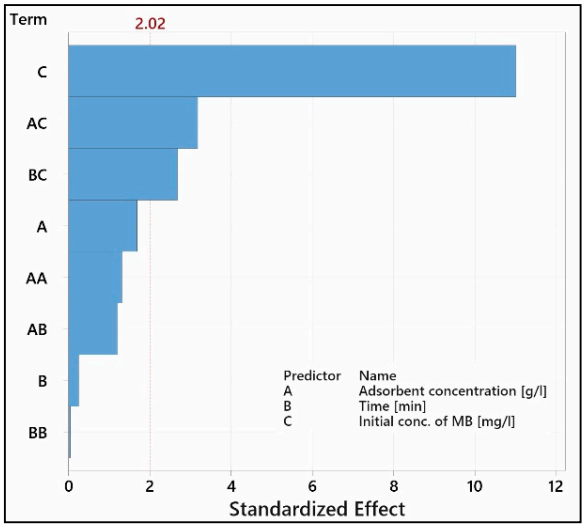


Figure 3. Pareto chart of the standardized effects.

From the Pareto chart (Figure 3), it can be seen that there is not a large number of parameters that have influence on the efficiency of MB removal, as only a few factors exceed the red significance threshold line (2.02), indicating statistical relevance. The initial concentration of MB (C) has by far the greatest influence, while the mutual interaction of the adsorbent concentration and the initial concentration of MB (AC) and the mutual interaction of time and the initial concentration of MB (BC) have smaller, but significant, influences. Other parameters have no significant influence on color removal. It is also observed that time (B) and the square of time (BB) have almost no influence on the adsorption process; that is, there is no great difference in efficiency between the lowest time in the study (10 min) and the highest (90 min). This is in agreement with other studies, in which the adsorption process was also found to be most intense at the beginning [6]. Therefore, in the following

studies, it is necessary to take smaller times (e.g., 2, 4, 6, 8 min) into consideration, because adsorption is most intense in the first 10 min.

3.3. Investigation of Adsorption Kinetics

In order to determine the order of the adsorption's kinetic model, an additional analysis was performed. By reviewing the literature data, it was established that adsorption can follow the pseudo-first-order or pseudo-second-order kinetic model. Accordingly, a comparison was made of the results for the two different initial concentrations of MB (12.5 mg/L and 25 mg/L) when the concentration of added adsorbent was 0.05 g/L. The results are shown in Figure 4.

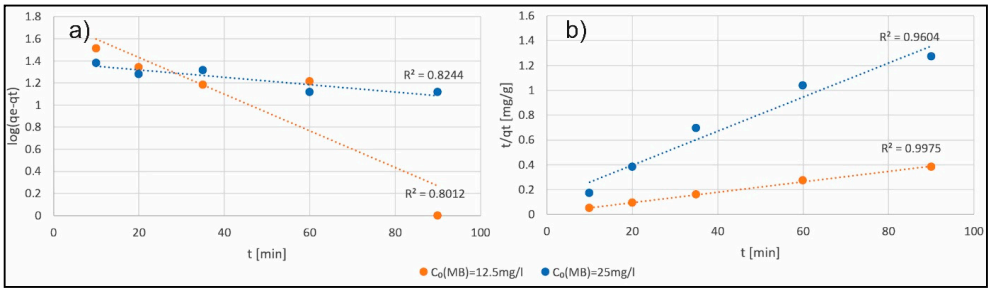


Figure 4. Comparison of MB adsorption kinetics of 0.05 g/L of adsorbent with initial MB concentrations of 12.5 mg/L and 25 mg/L: (**a**) pseudo-first order, (**b**) pseudo-second order.

From Figure 4, it can be seen that there are significant differences in the degree of correlation in the results. First of all, a low degree of correlation was observed for the pseudo-first-order model: R^2 = 0.8012 at an initial concentration of 12.5 mg/L MB, while for 25 mg/L MB it was still low and amounted to R^2 = 0.8244. The degree of correlation for the pseudo-second-order model were significantly higher: 0.9975 for the initial MB concentration of 12.5 mg/L, and 0.9604 for 25 mg/L of MB. Given that the degree of pseudo-second-order correlation is greater than 0.95, the adsorption of MB on activated carbon is considered to follow the pseudo-second-order kinetic model. In view of this, the adsorption rate is controlled by chemical interactions (such as the formation of hydrogen bonds or reactions between functional groups) between the adsorbent and the adsorbate (MB) [41]. Given that they are chemically compatible, adsorption can be improved with an increase in the dose of the adsorbent (an increase in the number of active sites available).

Figure 5 shows the adsorption kinetics of MB on activated carbon at different concentrations of active carbon.

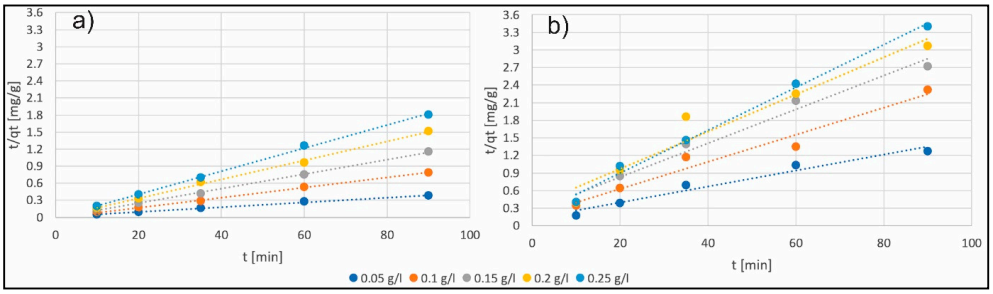


Figure 5. Results of adsorption kinetics at (**a**) initial MB concentration of 12.5 mg/L and (**b**) initial MB concentration of 25 mg/L.

Based on the previous diagrams, the degree of correlation and the corresponding coefficients for the pseudo-second-order equation are determined. For their determination, Equation (4) is used to plot the dependence of t/q_t on t. Using the curve of the graph, the slope and intercept are first determined. According to the equation, the slope of the

graph is $1/q_e$, while the intercept on the y-axis is $1/(k_2 \cdot q_e^2)$. Finally, based on the known slope ($q_e = 1/slope$), q_e is determined, and after obtaining q_e, k_2 is easily calculated using the formula $k_2 = 1/(intercept \cdot q_e^2)$. The results are shown in Table 1.

Table 1. Coefficients in the pseudo-second-order equation.

Adsorbent Conc. [g/L]	Equation	Slope	Intercept	q_e [mg/g]	k_2 [g/(mg·min)]	R^2
12.5 mg/L						
0.05	$t/q_t = 0.0110 + 0.0042t$	0.0042	0.0110	238.10	0.00160	0.9975
0.1	$t/q_t = 0.0052 + 0.0088t$	0.0088	0.0052	113.64	0.01489	0.9989
0.15	$t/q_t = 0.0084 + 0.0128t$	0.0128	0.0084	78.13	0.01950	0.9989
0.2	$t/q_t = 0.0018 + 0.0166t$	0.0166	0.0018	60.24	0.15309	0.9974
0.25	$t/q_t = 0.0022 + 0.0202t$	0.0202	0.0022	49.50	0.18547	0.9987
25 mg/L						
0.05	$t/q_t = 0.1220 + 0.0137t$	0.0137	0.1220	72.99	0.00154	0.9604
0.1	$t/q_t = 0.1720 + 0.0231t$	0.0231	0.1720	43.29	0.00310	0.9622
0.15	$t/q_t = 0.2571 + 0.0288t$	0.0288	0.2571	34.72	0.00323	0.9774
0.2	$t/q_t = 0.3389 + 0.0317t$	0.0317	0.3389	31.55	0.00297	0.9437
0.25	$t/q_t = 0.1708 + 0.0365t$	0.0365	0.1708	27.40	0.00780	0.9934

As for the equilibrium capacity (q_e), it can be seen from Table 1 that it decreases with an increase in the amount of adsorbent used in the case of both lower and higher initial concentrations of MB. For example, at an MB concentration of 12.5 mg/L, q_e decreases from 238.10 mg/g to 49.50 mg/g as the adsorbent concentration increases from 0.05 g/L to 0.25 g/L. At a higher adsorbent concentration, there are more active sites available, but the amount of the adsorbate that can be adsorbed per unit of adsorbent mass decreases. The rate constant k_2 increases with increasing adsorbent concentration (k_2 = 0.00160 g/mg·min at 0.05 g/L, k_2 = 0.18547 g/(mg·min) at 0.25 g/L). This is also in accordance with our previous considerations, because with an increase in the amount of adsorbent, the availability of active sites is greater, which leads to an increase in the rate of adsorption.

The equilibrium capacities (q_e) and rate constants (k_2) decrease with an increase in the concentration of MB. For example, for 12.5 mg/L of MB, q_e is 78.13 mg/g and k_2 is 0.01950 g/(mg·min), while for 25 mg/L, q_e is 34.72 mg/g and k_2 is 0.00323 g/(mg·min) (the active carbon concentration is 0.15 g/L in both cases). The reason for such a phenomenon is that a higher concentration of adsorbate leads to an increase in competition for the available adsorption sites. The degree of correlation, R^2, when testing pseudo-second-order kinetics is high at an MB concentration of 12.5 mg/L ($R^2 > 0.997$), while it is slightly lower for 25 mg/L of MB ($R^2 \approx 0.96$).

4. Conclusions

Research has shown that using activated carbon as an adsorbent achieves a high degree of removal of methylene blue from aqueous solutions. The results of our statistical analysis indicate that the greatest removal is achieved at lower initial dye concentrations and higher doses of adsorbent, while adsorption is most intense in the first 10 min. Activated carbon has a heterogeneous distribution of particle sizes, which is why it is possible to achieve easier filtration (due to larger particles) and a high adsorption efficiency (due to small particles with a large specific surface area). The process is of a pseudo-second order, which indicates that chemical interactions between the adsorbent and adsorbate are most important in the adsorption process. In future studies, optimization over shorter contact times is needed. This would further increase the efficiency of color removal and improve its practical ap-

plication in wastewater treatment. It is also necessary to integrate activated carbon into existing wastewater treatment systems, either as a standalone adsorbent or in combination with advanced oxidation processes. In addition, further research on the regeneration of activated carbon is needed to increase its cost-effectiveness for large-scale implementation.

Author Contributions: Conceptualization, N.V. and V.M.; methodology, N.V. and G.T.; software, N.V.; validation, V.M. and S.P.; formal analysis, J.V.; investigation, N.N.; resources, V.M. and N.V.; data curation, S.P.; writing—original draft preparation, G.T. and J.V.; writing—review and editing, G.T. and V.M.; visualization, N.N.; supervision, V.M. All authors have read and agreed to the published version of the manuscript.

Funding: This research received no external funding.

Institutional Review Board Statement: Not applicable.

Informed Consent Statement: Not applicable.

Data Availability Statement: Data are contained within the article.

Conflicts of Interest: The authors declare no conflicts of interest.

References

1. Ramutshatsha-Makhwedzha, D.; Mavhungu, A.; Moropeng, M.L.; Mbaya, R. Activated Carbon Derived from Waste Orange and Lemon Peels for the Adsorption of Methyl Orange and Methylene Blue Dyes from Wastewater. *Heliyon* **2022**, *8*, e09930. [CrossRef] [PubMed]
2. Kamdod, A.S.; Pavan Kumar, M.V. Adsorption of Methylene Blue and Methyl Orange on Tamarind Seed Activated Carbon and Its Composite with Chitosan: Equilibrium and Kinetic Studies. *Desal. Water Treat.* **2022**, *252*, 408–419. [CrossRef]
3. Waisi, B.I.; Al-Furaiji, M.H.; McCutcheon, J.R. Activated Carbon Nanofibers Nonwoven Flat Sheet for Methylene Blue Dye Adsorption: Batch and Flow-through Systems. *Desal. Water Treat.* **2023**, *289*, 228–237. [CrossRef]
4. Pan, X.; Zhao, N.; Shi, H.; Wang, H.; Ruan, F.; Wang, H.; Feng, Q. Biomass Activated Carbon Derived from Golden Needle Mushroom Root for the Methylene Blue and Methyl Orange Adsorption from Wastewater. *Ind. Crops Prod.* **2025**, *223*, 120051. [CrossRef]
5. Mechati, F.; Djilani, C.; Bougdah, N.; Messikh, N.; Boussaha, E.; Moumen, A.; Bouchalta, C.; Medjram, M.S. Adsorption of Methylene Blue onto Activated Carbon Prepared under N_2 /Microwave Radiation Supported Cobalt: Kinetics, Isotherms, and Thermodynamics Studies. *Desal. Water Treat.* **2023**, *284*, 288–300. [CrossRef]
6. Somsiripan, T.; Sangwichien, C. Enhancement of Adsorption Capacity of Methylene Blue, Malachite Green, and Rhodamine B onto KOH Activated Carbon Derived from Oil Palm Empty Fruit Bunches. *Arab. J. Chem.* **2023**, *16*, 105270. [CrossRef]
7. Jawad, A.H.; Sauodi, M.H.; Mastuli, M.S.; Aouda, M.A.; Radzun, K.A. Pomegranate Peels Collected from Fresh Juice Shop as a Renewable Precursor for High Surface Area Activated Carbon with Potential Application for Methylene Blue Adsorption. *Desal. Water Treat.* **2018**, *124*, 287–296. [CrossRef]
8. Dimbo, D.; Abewaa, M.; Adino, E.; Mengistu, A.; Takele, T.; Oro, A.; Rangaraju, M. Methylene Blue Adsorption from Aqueous Solution Using Activated Carbon of *Spathodea campanulata*. *Results Eng.* **2024**, *21*, 101910. [CrossRef]
9. Khebli, Z.; Djardire, R.; Boulkrinat, A.; Bouzerara, F. Elaboration of Zirconia Microfiltration Membranes Tested with Methylene Blue Filtration. *Desal. Water Treat.* **2022**, *279*, 4–7. [CrossRef]
10. Sotelo, S.; Oyarce, E.; Roa, K.; Boulett, A.; Pizarro, G.; Sánchez, J. Sodium Lignosulfonate as an Extracting Agent of Methylene Blue Dye Using a Polymer-Enhanced Ultrafiltration Technique. *Int. J. Biol. Macromol.* **2024**, *275*, 133567. [CrossRef]
11. Moghazy, R.M.; Mahmoud, R.H. Microalgal-Based Macro-Hollow Loofah Fiber Bio-Composite for Methylene Blue Removal: A Promising Step for a Green Adsorbent. *Int. J. Biol. Macromol.* **2023**, *253*, 127009. [CrossRef] [PubMed]
12. Ihaddaden, S.; Aberkane, D.; Boukerroui, A.; Robert, D. Removal of Methylene Blue (Basic Dye) by Coagulation-Flocculation with Biomaterials (Bentonite and *Opuntia ficus indica*). *J. Water Process Eng.* **2022**, *49*, 102952. [CrossRef]
13. Jiao, R.; Lou, T.; Zhang, H.; Wang, X. Preparation of Starch-Acrylic Acid-Carboxymethyl Cellulose Copolymer and Its Flocculation Performance towards Methylene Blue. *Biochem. Eng. J.* **2022**, *187*, 108635. [CrossRef]
14. Hu, Z.; Guo, C.; Wang, P.; Guo, R.; Liu, X.; Tian, Y. Electrochemical Degradation of Methylene Blue by Pb Modified Porous SnO_2 Anode. *Chemosphere* **2022**, *305*, 135447. [CrossRef]
15. Settu, M.; Gnanamoorthy, G.; Thirugnanam, B.; Vengidusamy, N.; Alotaibi, M.A. Vanadium Nitride /Poly(0-Methoxy Aniline)-Poly(3,4-Ethylene Dioxythiophene) Interpenetrated into Nanocomposite for Efficient Photocatalytic Degradation of Methylene Blue and Enhanced Electrochemical Sensing of Mebendazole. *Biosens. Bioelectron. X* **2024**, *19*, 100508. [CrossRef]

16. Hadi, S.; Taheri, E.; Amin, M.M.; Fatehizadeh, A.; Gardas, R.L. Empirical Modeling and Kinetic Study of Methylene Blue Removal from Synthetic Wastewater by Activation of Persulfate with Heterogeneous Fenton-like Process. *J. Mol. Liq.* **2021**, *328*, 115408. [CrossRef]
17. Ma, D.Y.; Wang, X.H.; Song, C.; Wang, S.G.; Fan, M.H.; Li, X.M. Aerobic Granulation for Methylene Blue Biodegradation in a Sequencing Batch Reactor. *Desalination* **2011**, *276*, 233–238. [CrossRef]
18. Liu, W.; Liu, L.; Liu, C.; Hao, Y.; Yang, H.; Yuan, B.; Jiang, J. Methylene Blue Enhances the Anaerobic Decolorization and Detoxication of Azo Dye by *Shewanella Onediensis* MR-1. *Biochem. Eng. J.* **2016**, *110*, 115–124. [CrossRef]
19. Khan, M.; Ahmed, M.M.; Akhtar, M.N.; Sajid, M.; Riaz, N.N.; Asif, M.; Kashif, M.; Shabbir, B.; Ahmad, K.; Saeed, M.; et al. Fabrication of CuWO4@MIL-101 (Fe) Nanocomposite for Efficient OER and Photodegradation of Methylene Blue. *Heliyon* **2024**, *10*, e40546. [CrossRef]
20. Balavinoth, M.; Sumithraj Premkumar, P.; Ravi Samuel Raj, C.; Ilavarasi Jeyamalar, J. Synthesis and Characterization of Mesoporous MCM-41 from Oil Template for Effective Adsorption of Methylene Blue Dye. *Phosphorus Sulfur Silicon Relat. Elem.* **2025**, *200*, 68–76. [CrossRef]
21. Dwivedi, P.; Rathore, A.K.; Srivastava, D.; Vijayakumar, R.P. Mechanistic Impact of Sodium Nitrate on the Characteristics of MWCNTS Oxidation and Potential Application on Methylene Blue Adsorption from Wastewater. *Waste Manag. Bull.* **2025**, *3*, 207–218. [CrossRef]
22. Misran, E.; Supardan, M.D.; Iryani, D.A.; Pramananda, V.; Sihombing, A.F.; Sitorus, D.V. Ultrasonic Assisted Adsorption of Methylene Blue Using Blood Clam Shell as a Low-Cost Adsorbent. *Results Eng.* **2024**, *23*, 102715. [CrossRef]
23. Borghei, S.A.; Zare, M.H.; Ahmadi, M.; Sadeghi, M.H.; Marjani, A.; Shirazian, S.; Ghadiri, M. Synthesis of Multi-Application Activated Carbon from Oak Seeds by KOH Activation for Methylene Blue Adsorption and Electrochemical Supercapacitor Electrode. *Arab. J. Chem.* **2021**, *14*, 102958. [CrossRef]
24. Francoeur, M.; Yacou, C.; Jean-Marius, C.; Chérémond, Y.; Jauregui-Haza, U.; Gaspard, S. Optimization of the Synthesis of Activated Carbon Prepared from *Sargassum* (sp.) and Its Use for Tetracycline, Penicillin, Caffeine and Methylene Blue Adsorption from Contaminated Water. *Environ. Technol. Innov.* **2022**, *28*, 102940. [CrossRef]
25. Iqajtaoune, A.; Taibi, M.; Saufi, H.; Aouan, B.; Boudad, L. Enhanced Removal of Methylene Blue and Procion Deep Red H-EXL Dyes from Aqueous Environments by Modified-Bentonite: Isotherm, Kinetic, and Thermodynamic. *Desal. Water Treat.* **2024**, *320*, 100607. [CrossRef]
26. Hayfron, J.; Jääskeläinen, S.; Tetteh, S. Synthesis of Zeolite from Rice Husk Ash and Kaolinite Clay for the Removal of Methylene Blue from Aqueous Solution. *Heliyon* **2025**, *11*, e41325. [CrossRef]
27. Al-Marri, A.H.; Moulahi, A.; Mogharbel, A.T.; Al-Mohaimeed, A.M.; Janene, F.; Ouda, A.S.; Al-Farraj, E.S.; Almaslamani, M.N.; Almaslamani, M.A.; Mjejri, I. Photocatalytic Performance of Nb2O5-Graphene Heterojunction for the Degradation of Methylene Blue. *Polyhedron* **2024**, *260*, 117080. [CrossRef]
28. Dolas, H. Activated Carbon Synthesis and Methylene Blue Adsorption from Pepper Stem Using Microwave Assisted Impregnation Method: Isotherm and Kinetics. *J. King Saud Univ. Sci.* **2023**, *35*, 102559. [CrossRef]
29. Zakaria, R.; Jamalluddin, N.A.; Abu Bakar, M.Z. Effect of Impregnation Ratio and Activation Temperature on the Yield and Adsorption Performance of Mangrove Based Activated Carbon for Methylene Blue Removal. *Results Mater.* **2021**, *10*, 102559. [CrossRef]
30. Wang, Y.; Pan, J.; Li, Y.; Zhang, P.; Li, M.; Zheng, H.; Zhang, X.; Li, H.; Du, Q. Methylene Blue Adsorption by Activated Carbon, Nickel Alginate/Activated Carbon Aerogel, and Nickel Alginate/Graphene Oxide Aerogel: A Comparison Study. *J. Mater. Res. Technol.* **2020**, *9*, 12443–12460. [CrossRef]
31. Bih, N.L.; Rwiza, M.J.; Ripanda, A.S.; Mahamat, A.A.; Machunda, R.L.; Choi, J.W. Adsorption of Phenol and Methylene Blue Contaminants onto High-Performance Catalytic Activated Carbon from Biomass Residues. *Heliyon* **2025**, *11*, e41150. [CrossRef] [PubMed]
32. Medhat, A.; El-Maghrabi, H.H.; Abdelghany, A.; Abdel Menem, N.M.; Raynaud, P.; Moustafa, Y.M.; Elsayed, M.A.; Nada, A.A. Efficiently Activated Carbons from Corn Cob for Methylene Blue Adsorption. *Appl. Surf. Sci. Adv.* **2021**, *3*, 100037. [CrossRef]
33. Oun, A.A.; Kamal, K.H.; Farroh, K.; Ali, E.F.; Hassan, M.A. Development of Fast and High-efficiency Sponge-gourd Fibers (Luffa Cylindrica)/Hydroxyapatite Composites for Removal of Lead and Methylene Blue. *Arab. J. Chem.* **2021**, *14*, 103281. [CrossRef]
34. Lagergren, S. Zur Theorie der sogenannten Adsorption gelöster Stoffe. *Z. Chem. Ind. Kolloide* **1907**, *2*, 15. [CrossRef]
35. Ho, Y.S.; McKay, G. Pseudo-second Order Model for Sorption Processes. *Process Biochem.* **1999**, *34*, 451–465. [CrossRef]
36. Hussain, O.A.; Hathout, A.S.; Abdel-Mobdy, Y.E.; Rashed, M.M.; Abdel Rahim, E.A.; Fouzy, A.S.M. Preparation and Characterization of Activated Carbon from Agricultural Wastes and their Ability to Remove Chlorpyrifos from Water. *Toxicol. Rep.* **2023**, *10*, 146–154. [CrossRef]
37. Verdoorn, D.S.; Zuliani, A.; Ranjan, P.J.; Holgado, P.; Khiar, N.; Saya, J.M.; Carrillo-Carrión, C.; Maes, B.U.W.; Orru, R.V.A. Unveiling the Potential of a Cobalt-Based Metal-Organic Framework in Carbodiimide Synthesis. *Adv. Synth. Catal.* **2025**, *367*, e202401540. [CrossRef]

38. Miura, H.; Sasaki, S.; Ogawa, R.; Shishido, T. Hydrosilylation of Allenes Over Palladium–Gold Alloy Catalysts: Enhancing Activity and Switching Selectivity by the Incorporation of Palladium into Gold Nanoparticles. *Eur. J. Org. Chem.* **2018**, *2018*, 1858–1862. [CrossRef]
39. Kaczmarski, K.; Przywara, M.; Lorenc-Grabowska, E. Advanced Modelling of Adsorption Process on Activated Carbon. *Chem. Eng. Res. Des.* **2022**, *181*, 27–40. [CrossRef]
40. Mustapha, L.S.; Kolade, S.O.; Durosinmi, S.O.; Tan, I.S.; Lau, S.Y.; Obayomi, K.S. Anthill Clay Activated *Ocimum Gratissimum* Extract for Effective Adsorption of Methylene Blue and Chromium (VI) Ion from Wastewater: Insights into the Adsorption Isotherms, Kinetics, Thermodynamics, and Mechanisms. *J. Water Process. Eng.* **2024**, *67*, 106286. [CrossRef]
41. Rao Vaddi, D.; Malla, R.; Geddapu, S. Magnetic Activated Carbon: A Promising Approach for the Removal of Methylene Blue from Wastewater. *Desal. Water Treat.* **2024**, *317*, 100146. [CrossRef]

Disclaimer/Publisher's Note: The statements, opinions and data contained in all publications are solely those of the individual author(s) and contributor(s) and not of MDPI and/or the editor(s). MDPI and/or the editor(s) disclaim responsibility for any injury to people or property resulting from any ideas, methods, instructions or products referred to in the content.